C. R. Mecanique 341 (2013) 161–170

Contents lists available at SciVerse ScienceDirect

Comptes Rendus Mecanique

www.sciencedirect.com

Combustion, flow and spray dynamics for aerospace propulsion

A comparison of the damping properties of perforated plates backed by a cavity operating at low and high Strouhal numbers

Alessandro Scarpato [a,b,*], Sébastien Ducruix [a,b], Thierry Schuller [a,b]

[a] CNRS, UPR 288, Laboratoire d'Énergétique Moléculaire et Macroscopique, Combustion (EM2C), 92295 Châtenay-Malabry, France
[b] École Centrale Paris, 92295 Châtenay-Malabry, France

ARTICLE INFO

Article history:
Available online 10 January 2013

Keywords:
Robust control
Perforated plate
Acoustic damping
Thermo-acoustic instabilities
Sound absorption

Mots-clés :
Contrôle robuste
Plaque perforée
Amortissement acoustique
Instabilités de combustion
Absorption sonore

ABSTRACT

Liners backed by a resonant cavity and traversed by a bias flow are widely used for acoustic damping in aeronautical engines. Their design relies on a relatively complex optimization procedure with a large number of parameters to examine. It is shown in this study how to reduce this number by maximizing absorption in two limit regimes where the choice of the optimal bias flow velocity and size of the back cavity can be decoupled. These developments apply for perforated plates of different porosity and thickness in the absence of grazing flow. In these regimes, the optimal bias flow velocity is only controlled by the plate porosity while the size of the back cavity fixes the peak absorption frequency. The first absorption regime reached at high Strouhal numbers is characterized by a Helmholtz resonance ($He \ll 1$) and a narrow frequency absorption bandwidth. The Mach number associated to the optimal bias flow velocity is then given by $M_c = (2/\pi)\sigma$, where σ is the plate porosity. This regime minimizes the size of the resonant back cavity, but the absorption bandwidth narrows also with the Strouhal number. The second absorption regime reached at low Strouhal numbers operates with a quarter-wave resonator ($He \simeq \pi/2$) and a bias flow velocity fixed by $M_c = \sigma/2$. This regime offers a wide absorption bandwidth around the peak absorption frequency well suited for low frequency dampers when the bias flow velocity may vary within the system. Theoretical expressions derived in this study are validated against experimental data in the two regimes identified. They may be used to ease the design of robust dampers to hinder self-sustained thermo-acoustic instabilities when the instability frequency varies.

RÉSUMÉ

Les plaques perforées couplées à une cavité résonante et traversées par un écoulement axial sont souvent utilisées pour augmenter l'amortissement acoustique dans les moteurs aéronautiques. Leur conception repose sur une procédure d'optimisation complexe, avec un jeu important de paramètres à examiner. Dans cette étude nous montrons comment réduire ce nombre de paramètres en maximisant l'absorption dans deux régimes asymptotiques où les choix de la vitesse optimale dans les trous et de la taille de la cavité résonante peuvent être découplés. Des expressions analytiques utiles lors de la conception sont indiquées pour ces deux régimes de fonctionnement caractérisés par des bandes d'absorption étroite à fort Strouhal et large à faible Strouhal. Ces développements sont valides pour des plaques perforées de différentes porosités et épaisseurs en absence d'écoulement rasant. Ils

* Corresponding author at: CNRS, UPR 288, Laboratoire d'Énergétique Moléculaire et Macroscopique, Combustion (EM2C), 92295 Châtenay-Malabry, France.
E-mail addresses: alessandro.scarpato@ecp.fr (A. Scarpato), sebastien.ducruix@ecp.fr (S. Ducruix), thierry.schuller@ecp.fr (T. Schuller).

1631-0721/$ – see front matter
http://dx.doi.org/10.1016/j.crme.2012.10.016

peuvent contribuer à améliorer la conception de systèmes robustes d'atténuation d'instabilités de combustion lorsque la fréquence de l'instabilité varie.

1. Introduction

Acoustic dampers based on perforated screens backed by a cavity and traversed by a bias flow are a widely used technological solution, capable to damp both high frequency transverse modes associated to screech-tone noise in afterburners [1] and low frequency thermo-acoustic instabilities in gas turbine combustion chambers [2]. Lörstad et al. [3] showed that the introduction of wall perforations located near the burners of an industrial gas turbine combustor significantly increased the acoustic damping of the system. Richards et al. [4] also highlighted the importance of the design of robust resonators in a combustion chamber, since damping performances may vary with operating conditions.

Modeling the acoustic response of these dampers is an ongoing issue tackled by different approaches, like those introduced by Ingard and Ising [5], Cummings [6–8], Melling [9] and Howe [10]. A number of parameters influence the absorption properties of perforates, such as the porosity [11], the plate thickness [12,13], the orifice geometry [14], the interspace between holes [15,16], the presence of bias and grazing flows [17,18] as well as the sound pressure level [19,20]. The design of a perforated plate used as a damper relies thus on a complex optimization procedure, involving a large number of parameters to examine.

In the present work conditions that maximize acoustic absorption of a perforated plate backed by a cavity are determined by finding the parameters that set the reflection coefficient to zero. The analysis is limited to small disturbance levels for perforated plates traversed by a mean bias flow in the absence of a grazing flow. Two interesting asymptotic regimes are identified, which are reached at low and high Strouhal numbers $\mathrm{St} = \omega a/\bar{u}_0$ calculated with the perforation radius a, bias flow velocity $\bar{u}_0$ and peak absorption angular frequency ω. By operating in these conditions, it is shown that it is possible to decouple the choice of the optimal bias flow velocity in the orifices $\bar{u}_0$ and the back cavity depth L to maximize absorption for plates featuring different thickness h.

After a brief presentation in Section 2 of the models used to analyze the damping properties of perforated plates, conditions maximizing absorption in presence of a resonant back cavity are examined in Section 3.

The high Strouhal optimal regime is analyzed first in Section 3.1. It is characterized by a Helmholtz resonance taking place in the back cavity, where maximum absorption is reached for small Helmholtz numbers $\mathrm{He} = kL \ll 1$, k being the wavenumber and L the size of the back cavity. Conditions that must be satisfied by the bias flow velocity in this regime are derived. An analysis of the absorption bandwidth around the peak absorption frequency is then conducted. Advantages and drawbacks of working in this optimal absorption regime are also discussed.

Rupp et al. [21] recently showed that in modern combustion chambers, dampers based on perforated plates operate at small Strouhal numbers, $\mathrm{St} \leqslant 0.25$. Absorption properties in the low Strouhal regime were analyzed in a recent work [22] for infinitely thin plates. It was shown in this case that the size of the back cavity must be tuned to be close to a quarter-wave resonator to maximize absorption: $\mathrm{He} \simeq \pi/2$. In the present work effects of plate thickness are included in the analysis. It is shown in Section 3.2 that this regime features a large frequency bandwidth around the peak absorption frequency well suited for the design of robust low frequency dampers. These theoretical elements are completed in Section 4 by comparisons with measurements found in the literature for the low and high Strouhal regimes identified in this work.

2. Acoustic absorption of perforates with a back cavity

As shown by Morfey [23], acoustic energy can be dissipated in a vortical flow. When a bias flow passes through an orifice of a perforated plate, it separates as a jet, constituting a source of vorticity. A fraction of the acoustic energy of the incident sound waves is thus converted into vortical energy, which is then dissipated by viscous losses [24]. In the absence of bias flow through the perforations, absorption only takes place at high sound levels when acoustic waves propagating in the quiescent flow produce large vortices at the perforation outlets [5–9,19,20]. By adding a small bias velocity in the perforations, flow separation induced by the jet promotes the generation of vorticity and enhances acoustic absorption. In this latter case, sound absorption is a linear mechanism [10], and this will be the regime examined in this study.

Consider the geometrical configuration described in Fig. 1. A perforated plate backed by a cavity of depth L and traversed by a mean bias flow is submitted to normal incident sound waves. Circular orifices of diameter $2a$ are arranged in a square pattern, with an interhole distance d. Assuming that only harmonic plane waves propagate in the duct, fluctuations can be decomposed as $y(x,t) = \tilde{y}(x)\exp(-\mathrm{i}\omega t)$, where ω is the angular frequency. The analysis developed in this section follows that of Hughes and Dowling [1], but different dimensionless numbers are used to analyze the resulting expressions. The acoustic pressure and velocity in the cavity can be expressed as follows:

$$\tilde{p}_-(x) = A\exp(\mathrm{i}kx) + B\exp(-\mathrm{i}kx) \tag{1}$$

$$\rho_0 c_0 \tilde{u}_-(x) = A\exp(\mathrm{i}kx) - B\exp(-\mathrm{i}kx) \tag{2}$$

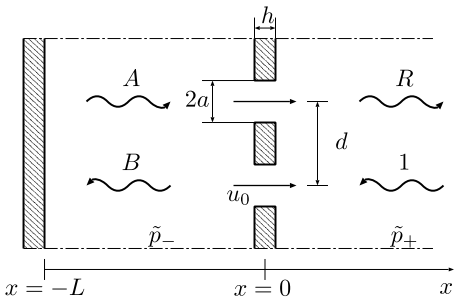

Fig. 1. Perforated plate backed by a resonant cavity, traversed by a mean bias flow and submitted to normal sound waves.

where $-L \leqslant x \leqslant 0$, ρ_0 is the mean density, c_0 is the speed of sound and $k = \omega/c_0$ is the wavenumber. Outside the cavity, one obtains:

$$\tilde{p}_+(x) = R\exp(\mathrm{i}kx) + \exp(-\mathrm{i}kx) \tag{3}$$

$$\rho_0 c_0 \tilde{u}_+(x) = R\exp(\mathrm{i}kx) - \exp(-\mathrm{i}kx) \tag{4}$$

In these expressions, A, B and R are the complex amplitudes of the sound waves. Three conditions are necessary to obtain an expression for the reflection coefficient R. The first is given by the continuity of the acoustic volume flowrate $\tilde{q}$ near the perforation $x = 0$ for a compact plate:

$$\tilde{q}(0) = \tilde{u}_-(0)d^2 = \tilde{u}_0\pi a^2 = \tilde{u}_+(0)d^2 \tag{5}$$

The acoustic pressure difference applied to the plate generates an unsteady volumetric flowrate determined by the Rayleigh conductivity of the perforation [18,25]:

$$\mathrm{i}\rho_0\omega\pi a^2\tilde{u}_0 = K_R\big[\tilde{p}_+(0) - \tilde{p}_-(0)\big] \tag{6}$$

Equations (5) and (6), together with the rigid wall condition $\tilde{u}_-(-L) = 0$ at the back-cavity rear side, allow to obtain an expression for the specific impedance $\zeta = \tilde{p}_+/\rho_0 c_0 \tilde{u}_+$ at the plate location $x = 0^+$:

$$\zeta = \mathrm{i}\left[\frac{kd^2}{K_R} - \frac{1}{\tan(\mathrm{He})}\right] \tag{7}$$

where $\mathrm{He} = kL$ is the Helmholtz number of the back cavity. Finally, the reflection coefficient writes:

$$R = \frac{\zeta + 1}{\zeta - 1} \tag{8}$$

The absorption coefficient can also be defined using the relation $\alpha = 1 - |R|^2$.

Equations (7) and (8) show that a model for the Rayleigh conductivity K_R is needed to fully characterize the reflection coefficient of a perforated plate. Howe [10] showed that, when a cylindrical vortex sheet is shed at the orifice outlet and is convected downstream at a constant velocity u_c, the Rayleigh conductivity K_R is given by:

$$K_R = 2a(\gamma - \mathrm{i}\delta) \tag{9}$$

where γ and δ are functions of the Strouhal number $\mathrm{St} = \omega a/u_c$:

$$\gamma - \mathrm{i}\delta = 1 + \frac{(\pi/2)I_1(\mathrm{St})\exp(-\mathrm{St}) - \mathrm{i}K_1(\mathrm{St})\sinh(\mathrm{St})}{\mathrm{St}[(\pi/2)I_1(\mathrm{St})\exp(-\mathrm{St}) + \mathrm{i}K_1(\mathrm{St})\cosh(\mathrm{St})]} \tag{10}$$

In this expression, I_1 and K_1 are modified Bessel functions of the first and second kinds. It is now important to determine the convection velocity u_c. For quasi-steady operating conditions, Howe stated that the vorticity convection velocity u_c equals half the jet velocity [10]. Experiments [1,26] indicate that a convection velocity equal to the mean bias flow velocity in the orifice $u_c \simeq \bar{u}_0$ yields a better agreement between measurements and previsions. The same assumption $u_c = \bar{u}_0$ is made in the present study, but other relations could be used, leading to similar conclusions.

Equation (10) is valid for infinitely thin plates. Jing and Sun [12] developed a model taking into account the additional dissipation due to a finite plate of thickness h. In this case, the function $\gamma - \mathrm{i}\delta$ should be modified as follows:

$$\frac{1}{\gamma' - \mathrm{i}\delta'} = \frac{1}{\gamma - \mathrm{i}\delta} + \frac{2h}{\pi a} \tag{11}$$

Combining Eq. (9) with Eq. (7) one obtains an analytical expression for the specific impedance ζ of a perforated plate. With the introduction of the Mach number based on the convection velocity of the vortex sheet $\mathrm{M}_c = u_c/c_0$ and the

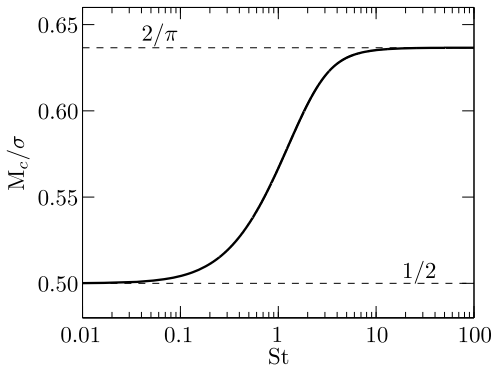

Fig. 2. Evolution of the optimal ratio M_c/σ as a function of the Strouhal number St, given by Eq. (16). This ratio is independent of the plate thickness.

plate porosity $\sigma = \pi a^2/d^2$, Eq. (7) determining the specific impedance of the system can be written as a function of four dimensionless numbers St, He, h/a and M_c/σ:

$$\zeta = \mathrm{i}\left[\frac{\pi}{2}\mathrm{St}\frac{M_c}{\sigma}\left(\frac{1}{\gamma - \mathrm{i}\delta} + \frac{2h}{\pi a}\right) - \frac{1}{\tan(\mathrm{He})}\right] \tag{12}$$

For the following analysis concerning small and large Strouhal number limits, it is interesting to note that the expression in Eq. (10) reduces to [18]:

$$\gamma - \mathrm{i}\delta \simeq \frac{\mathrm{St}^2}{3} - \mathrm{i}\frac{\pi\,\mathrm{St}}{4}, \quad \text{when } \mathrm{St} \ll 1 \tag{13}$$

$$\gamma - \mathrm{i}\delta \simeq 1 - \frac{\mathrm{i}}{\mathrm{St}}, \quad \text{when } \mathrm{St} \gg 1 \tag{14}$$

It is now worth analyzing conditions leading to optimal absorption. These expressions are used in the following section to identify two limit regimes at low and high Strouhal numbers with interesting damping properties.

3. Maximization of absorption

Maximum absorption is obtained by setting the reflection coefficient to zero $R = 0$. Equation (8) shows that this is equivalent to find the roots of $\zeta + 1 = 0$, i.e.:

$$\Re(\zeta) + 1 = 0 \quad \text{and} \quad \Im(\zeta) = 0 \tag{15}$$

where $\Re(\zeta)$ and $\Im(\zeta)$ indicate the real and imaginary components of the specific impedance. Using Eq. (12) in Eq. (15) one obtains the following set of conditions:

$$\frac{M_c}{\sigma} = \frac{2}{\pi\,\mathrm{St}}\frac{\gamma^2 + \delta^2}{\delta} \tag{16}$$

$$\frac{1}{\tan(\mathrm{He})} = \frac{\gamma}{\delta} + \frac{2h}{\pi a}\frac{\gamma^2 + \delta^2}{\delta} \tag{17}$$

Equation (16) fixes the optimal Mach number to porosity ratio M_c/σ corresponding to an anechoic condition $R = 0$. This ratio is a monotonically increasing function of the Strouhal number St, as shown in Fig. 2. This figure also indicates that values of M_c/σ are bounded by $1/2 \leqslant M_c/\sigma \leqslant 2/\pi$ for all Strouhal numbers. We will demonstrate in Sections 3.1 and 3.2 that these boundaries reached at low and high Strouhal numbers constitute particularly interesting operating regimes to design dampers.

The optimal Helmholtz number He of the back cavity is fixed by Eq. (17). For a plate of finite thickness h, this parameter depends on both the Strouhal number and the thickness to orifice radius ratio h/a. Note that for an infinitely thin plate, this expression reduces to $\tan(\mathrm{He}) = \delta/\gamma$, which is a function of the Strouhal number only. Fig. 3 shows that the Helmholtz number decreases monotonically when the Strouhal number increases: $\mathrm{He} \to \pi/2$ for $\mathrm{St} \ll 1$, and $\mathrm{He} \to 0$ when $\mathrm{St} \gg 1$. Increasing the plate thickness does not modify these limits, but intermediate values are shifted towards lower Strouhal numbers. The choice of the optimal bias flow velocity and back cavity depth are generally interrelated [1,26]. One possibility to ease the design of dampers is to identify regimes where these parameters can be fixed independently. This problem was not examined in previous investigations. It is the object of the following section.

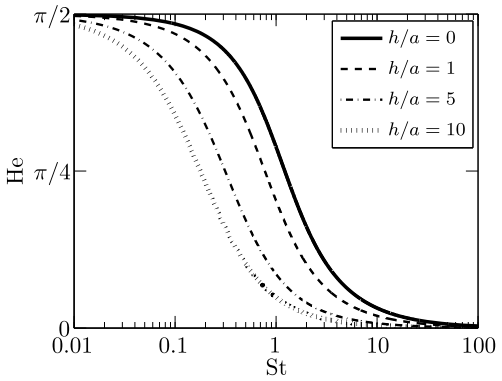

Fig. 3. Evolution of the optimal Helmholtz number He as a function of the Strouhal number St, given by Eq. (17) for different values of the thickness ratio $h/a = 0, 1, 5$ and 10.

3.1. Analysis at high Strouhal number

The first interesting regime is obtained for high values of the Strouhal number. Using the asymptotic form Eq. (14) to estimate the γ and δ functions at high Strouhal number $\mathrm{St} \gg 1$, Eqs. (16) and (17) reduce to:

$$\frac{\mathrm{M}_c}{\sigma} = \frac{2}{\pi} \tag{18}$$

$$\frac{1}{\tan(\mathrm{He})} = \mathrm{St}\left(1 + \frac{2h}{\pi a}\right) \tag{19}$$

This set of conditions can be used to design compact acoustic absorbers to damp a particular frequency. Equation (18) shows that, at large Strouhal numbers, the bias flow velocity is uniquely fixed by the plate porosity, and is given by $\bar{u}_0 = u_c = 2\sigma c_0/\pi$. Combining this expression with the knowledge of the frequency to damp, Eq. (19) defines the optimal Helmholtz number, and consequently determines also the optimal cavity depth L. Note that when $\mathrm{St} \gg 1$, Eq. (19) implies that $\tan(\mathrm{He}) \to 0$. The smallest Helmholtz number satisfying this condition is $\mathrm{He} = kL \simeq 0$. This model shows that operating at high Strouhal numbers enables to design compact dampers with short cavity depths.

It is now useful to introduce the resonance parameter Q, defined as the ratio between the angular frequency ω and the resonance frequency of a Helmholtz resonator $\omega_{\mathrm{He}} = (2ac_0^2/Ld^2)^{1/2}$ formed by the back cavity volume and the neck of the perforation:

$$\mathrm{Q} = \left(\frac{\omega}{\omega_{\mathrm{He}}}\right)^2 = \frac{\pi}{2}\mathrm{St}\frac{\mathrm{M}_c}{\sigma}\mathrm{He} \tag{20}$$

Hughes and Dowling [1] argued that, for infinitely thin plates, improved absorption properties are expected near Helmholtz resonance, and proposed to work at $\mathrm{Q} = 1$. Substituting Eq. (18) in Eq. (20) leads to $\mathrm{Q} = \mathrm{St}\,\mathrm{He}$. Operating with a Helmholtz resonator $\mathrm{He} \ll 1$ at $\mathrm{Q} = 1$ necessarily implies that the Strouhal number in the perforations takes large values $\mathrm{St} \gg 1$.

Fig. 4(a) plots the modulus of the reflection coefficient $|R|$ as a function of the Helmholtz number He, obtained by combining Eq. (8) with Eq. (12), at $\mathrm{St} = 5$ for an infinitely thin plate ($h/a = 0$) and for several values of the ratio M_c/σ. It is shown here that optimal absorption $R = 0$ is reached only for $\mathrm{M}_c/\sigma = 2/\pi$. When this condition is not met, absorption properties are degraded. The smallest value of the reflection coefficient increases, and maximum absorption is slightly shifted towards higher Helmholtz numbers when M_c/σ decreases. Conversely, when M_c/σ increases, the peak absorption is shifted towards lower values of the Helmholtz number. It is also interesting to note that maximum absorption occurs when the resonance condition $\mathrm{Q} = 1$ is met. In Fig. 4(a), the Strouhal number is fixed to $\mathrm{St} = 5$. For $\mathrm{M}_c/\sigma = 2/\pi$ the resonance parameter is thus a linear function of the Helmholtz number only $\mathrm{Q} = \mathrm{St}\,\mathrm{He}$. In the present case the Helmholtz number corresponding to the peak absorption is equal to $\mathrm{He} = \mathrm{Q}/\mathrm{St} = 1/5$.

Operating at $\mathrm{Q} = 1$ is not the best solution to maximize damping when the plate thickness cannot be neglected. Fig. 4(b) shows the modulus of the reflection coefficient plotted as a function of the Helmholtz number when $\mathrm{St} = 5$ and $\mathrm{M}_c/\sigma = 2/\pi$. When these parameters are fixed, increasing the plate thickness h degrades the absorption bandwidth of the perforate, and shifts the peak absorption towards lower Helmholtz numbers. It is possible to show that the effect of the plate thickness modifies the resonance condition of the cavity. Replacing the identity $\mathrm{Q} = \mathrm{St}\,\mathrm{He}$ in Eq. (19) leads to:

$$\frac{1}{\tan(\mathrm{He})} = \frac{\mathrm{Q}}{\mathrm{He}}\left(1 + \frac{2h}{\pi a}\right) \tag{21}$$

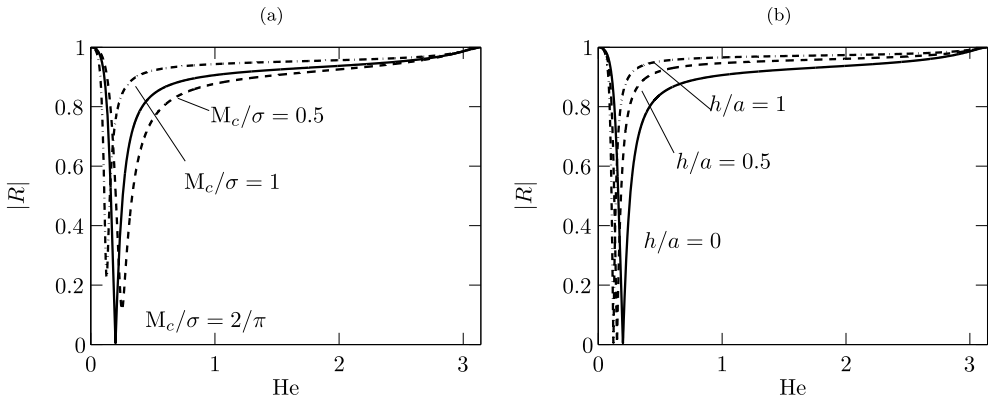

Fig. 4. Modulus $|R|$ of the reflection coefficient as a function of the Helmholtz number He, for a fixed Strouhal number $\mathrm{St} = 5$. (a): influence of the ratio M_c/σ for an infinitely thin plate, $h/a = 0$. (b): influence of the plate thickness h when $\mathrm{M}_c/\sigma = 2/\pi$.

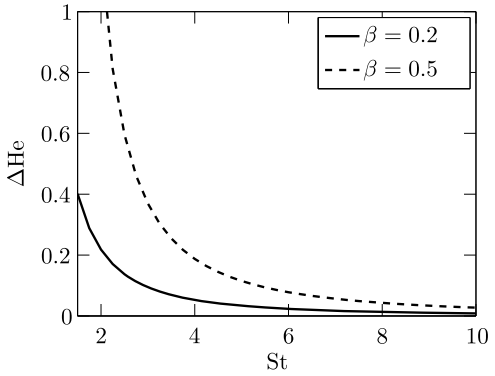

Fig. 5. Evolution of the range of Helmholtz numbers $\Delta\mathrm{He}$ satisfying $|R| \leqslant \beta$ as a function of the Strouhal number St, determined by Eq. (24) for different values of the threshold β and for an infinitely thin plate $h/a = 0$.

At high Strouhal numbers, maximum absorption is reached for $\mathrm{He} \ll 1$, implying that $\tan(\mathrm{He}) \simeq \mathrm{He}$. Optimal absorption at high Strouhal numbers for thick perforates is then defined by:

$$\mathrm{Q}\left(1 + \frac{2h}{\pi a}\right) = 1 \tag{22}$$

The resonant frequency of the back cavity depends on the effective length of the orifice, which is the sum of the plate thickness and the end correction accounting for the inertia of the mass of fluid oscillating in the orifice. When the plate thickness is of the order of the orifice radius a, Eq. (22) replaces the condition $\mathrm{Q} = 1$.

It is now interesting to analyze the absorption bandwidth around the peak absorption frequency in the high Strouhal regime identified in this study. First, an approximate equation for the reflection coefficient R is derived starting from Eqs. (8) and (12). Taking also the high Strouhal number limit expression for the Rayleigh conductivity given by Eq. (14) and the condition Eq. (18), one obtains:

$$\frac{1}{R} = 1 + \frac{2\mathrm{i}}{\mathrm{St}(1 + \frac{2h}{\pi a}) - \frac{1}{\tan(\mathrm{He})}} \tag{23}$$

The range of Helmholtz numbers $\Delta\mathrm{He}$ satisfying $|R| \leqslant \beta$, where $\beta \in [0, 1]$ is an arbitrary threshold level, can be determined by introducing the thickness parameter $\eta_h = 1 + 2h/(\pi a)$ and using the approximation $\tan(\mathrm{He}) \simeq \mathrm{He}$ valid near optimal absorption:

$$\Delta\mathrm{He} = \frac{4\beta(1-\beta^2)}{\eta_h^2 \mathrm{St}^2 (1-\beta^2)^2 - 4\beta^2} \tag{24}$$

Eq. (24) demonstrates that the absorption bandwidth $\Delta\mathrm{He}$ where $|R| \leqslant \beta$ is inversely proportional to the square of the Strouhal number. In the high Strouhal regime the absorption bandwidth narrows when St increases. This is shown in Fig. 5. For the sake of clarity, the absorption bandwidth $\Delta\mathrm{He}$ is plotted as a function of the Strouhal number only for an infinitely thin plate, but the same analysis holds for thick plates.

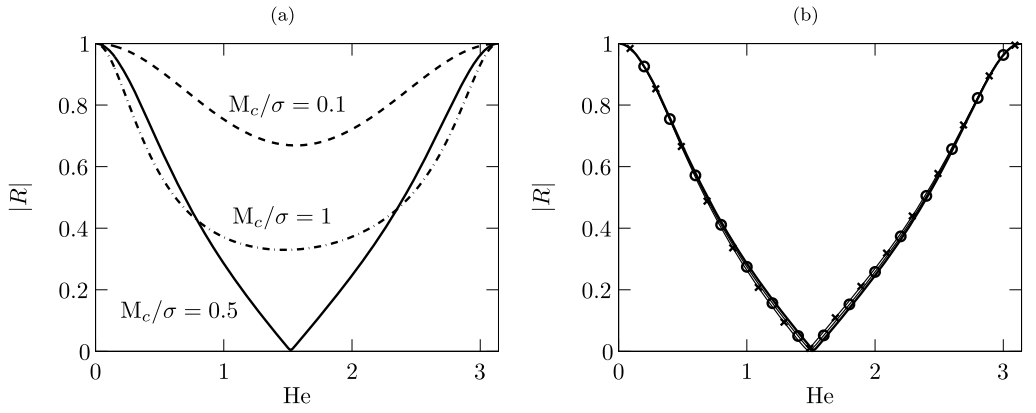

Fig. 6. Modulus $|R|$ of the reflection coefficient as a function of the Helmholtz number He, at $St = 0.1$. (a): influence of the ratio M_c/σ, at $h/a = 0$. (b): influence of the plate thickness h, at $M_c/\sigma = 0.5$. $h/a = 0$ (solid bold line), $h/a = 0.5$ (∘), $h/a = 1$ (×).

Operating with a Helmholtz resonator enables to reduce the size of the back cavity of the damper. The optimal size of the back cavity is set by $Q[1 + 2h/(\pi a)] = 1$, where Q denotes the resonance parameter which is fixed for a given geometry and frequency. The optimal bias flow velocity is fixed by the plate porosity $M_c/\sigma = 2/\pi$ and does not depend on frequency. The only requirement for the damper is to work at high Strouhal numbers. This regime is characterized by a narrow absorption bandwidth around peak absorption. In the next section a similar study is carried out on the second operating regime limit, when the Strouhal number takes small values.

3.2. Analysis at low Strouhal number

In modern aeronautical engine combustors, harmful unstable modes can range from a few tens to a few thousand pulsations per second, and the orifices present in the combustion chamber are generally small. These orifices are traversed by a bias flow with a relatively high velocity. Thus the Strouhal numbers in these orifices take also generally small values. It is not rare that the instability frequency and the damper performance vary with the operating regime [4,27,28]. Efficient dampers must then feature good absorption properties over a large range of frequencies. The low Strouhal asymptotic regime is analyzed in this section. It is shown that this regime fulfills conditions for robust damping at low frequencies.

In the limit of low Strouhal numbers, the asymptotic form Eq. (13) for the functions γ and δ can be replaced in Eqs. (16) and (17), which reduce to:

$$\frac{M_c}{\sigma} = \frac{1}{2} \tag{25}$$

$$\frac{1}{\tan(He)} = St\left(\frac{4}{3\pi} + \frac{h}{2a}\right) \tag{26}$$

The optimal bias flow velocity $\bar{u}_0$ in the perforations is in this regime again fixed by the plate porosity only, $\bar{u}_0 = u_c = \sigma c_0/2$. Equation (26) can then be used to fix the frequency to damp by adjusting the back cavity size L. It is worth noting that when $St \ll 1$, $\tan(He) \to \infty$ to satisfy Eq. (26), and thus $He \simeq \pi/2$. At low Strouhal numbers, optimal absorption is reached when the cavity operates as a quarter-wave resonator.

In Fig. 6(a) the modulus of the reflection coefficient $|R|$ is plotted as a function of the Helmholtz number He, when $St = 0.1$, for different values of the ratio M_c/σ. It is shown that maximum absorption is reached for $M_c/\sigma = 1/2$. Moving away from this optimal ratio does not change significantly the Helmholtz number corresponding to the peak absorption condition, but the smallest value taken by the reflection coefficient increases. Absorption properties are thus degraded.

The influence of plate thickness is shown in Fig. 6(b). In the low Strouhal number regime, effects of thickness are negligible, leading to a very slight shift of maximal absorption towards lower Helmholtz numbers when the plate thickness increases. This behavior is in agreement with the observations from Jing and Sun [12], who indicated that at high bias flow velocities, hence at low Strouhal numbers, the acoustic response of a thick perforate is barely modified compared to the response of the corresponding thin plate.

Fig. 6(a) suggests that in the low Strouhal regime the absorption bandwidth around the peak absorption frequency is large compared to the one found in the high Strouhal regime. It is possible to demonstrate it analytically. Starting from Eqs. (8) and (12), taking the limit $St \ll 1$ and the condition $M_c/\sigma = 1/2$ defined by Eq. (25), one obtains:

$$\frac{1}{R} = 1 + \frac{2i}{St(\frac{h}{2a} + \frac{4}{3\pi}) - \frac{1}{\tan(He)}} \tag{27}$$

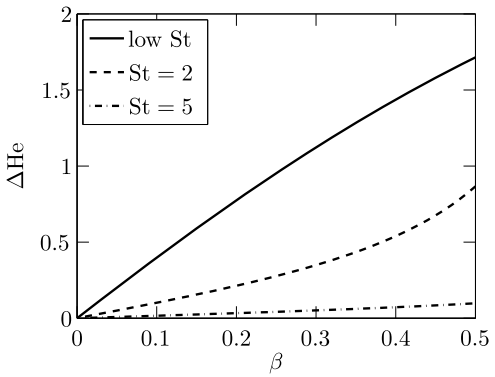

Fig. 7. Evolution of the range of Helmholtz numbers $\Delta\mathrm{He}$ where $|R| \leqslant \beta$ as a function of the threshold level β, in the low Strouhal regime defined by Eq. (28) (solid line), and in the high Strouhal regime defined by Eq. (24) (dashed and dashed–dotted lines), for an infinitely thin plate $h/a = 0$.

Table 1
Perforated plate parameters for the two configurations explored. a: aperture radius, σ: porosity, h: plate thickness, L: back cavity depth, σ: porosity, M_c: Mach number in the orifices.

Configuration	a [mm]	σ [%]	h [mm]	L [mm]	M_c/σ	Range of St
High Strouhal [1]	1.5	2.40	$\simeq 0$	10	0.57	0.97–5.82
Low Strouhal [22]	0.5	4.84	1	150	0.50	0.037–0.37

Following [22], Eq. (27) can be used to determine the absorption bandwidth $\Delta\mathrm{He}$, again defined as the range of Helmholtz numbers verifying $|R| \leqslant \beta$, $\beta \leqslant 1$ being an arbitrary threshold. In the small Strouhal limit $\mathrm{St} \ll 1$, one finally obtains:

$$\Delta\mathrm{He} = \pi - 2\arctan\left[\frac{1-\beta^2}{2\beta}\right] \tag{28}$$

Equation (28) shows that the absorption bandwidth at low Strouhal number depends only on the threshold level β. A comparison between the absorption bandwidth in the low and high Strouhal regimes analyzed in this study is presented in Fig. 7. It is interesting to note that the range of Helmholtz numbers over which optimized absorption properties are found is always larger for the low Strouhal regime than for the high Strouhal one.

In conclusion to this section, the low Strouhal regime features a large absorption bandwidth, which makes it suitable for the design of robust dampers. In this regime, the optimal bias flow velocity is only fixed by the plate porosity and is given by $\mathrm{M}_c/\sigma = 1/2$. However, the back cavity operates as a quarter-wave resonator, thus its depth will be larger than for a damper operating at high Strouhal numbers.

4. Comparison with experimental data

Experimental data for two different perforated plate configurations were selected in the literature [1,22] to validate the models described in this study operating in the low and high Strouhal regimes. Table 1 synthesizes the main parameters characterizing these operating regimes.

The first configuration examined is the one studied by Hughes and Dowling [1]. In the top graph of Fig. 6 in their paper, the absorption coefficient $\alpha = 1 - |R|^2$ is plotted as a function of the resonance parameter Q, for a constant back cavity depth L and Mach number M_c in the orifice. Note that in this configuration the range of Strouhal numbers investigated is quite high ($0.97 \leqslant \mathrm{St} \leqslant 5.82$, Table 1). Experimental data were extracted from [1] and are plotted in Fig. 8(a). These data are compared to predictions obtained with the high Strouhal approximation Eq. (23), and with the complete model obtained by combining Eqs. (8) and (12). Hughes and Dowling did not take into account the effect of plate thickness in their study, therefore these theoretical relations are computed by assuming $h/a = 0$. The agreement between both models and measurements is fairly good, although the peak absorption obtained with the high Strouhal approximation is predicted at a slightly lower frequency compared to the complete model and experimental data. It is also worth noting that maximum absorption $\alpha = 1$ or equivalently $|R| = 0$ is achievable in practice.

In the configuration explored in [22], the perforated plate operates in the low Strouhal regime. The hole radius is much smaller than in the first configuration, the back cavity depth is larger and the range of Strouhal numbers considered is lower ($0.037 \leqslant \mathrm{St} \leqslant 0.37$, Table 1). Experimental data were adapted from Fig. 13a in [22], and are presented in Fig. 8(b) for the absorption coefficient as a function of frequency. These measurements are compared to predictions determined with the low Strouhal approximation Eq. (27) and the complete model obtained by combining Eqs. (8) and (12). In [22] the thickness ratio was equal to $h/a = 2$. This effect was included in the predictions in Fig. 8(b). The agreement between the theoretical predictions and measurements is very good over the whole frequency range investigated $100 \leqslant f \leqslant 1000$ Hz.

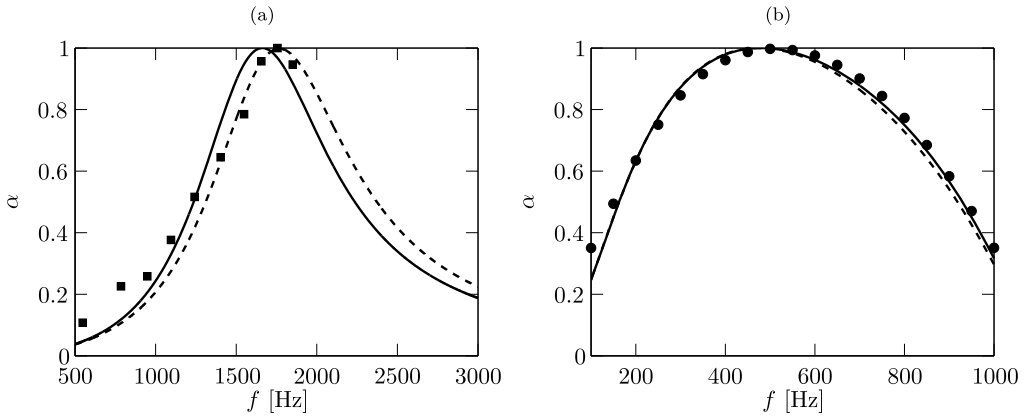

Fig. 8. Evolution of the absorption coefficient $\alpha = 1 - |R|^2$ as a function of frequency f. (a): data extracted from [1] (■) are compared to the high Strouhal model Eq. (23) with $h/a = 0$ (solid line), and to the complete model obtained by combining Eqs. (8) and (12) with $h/a = 0$ (dashed line). (b): data extracted from [22] (•) are compared to the low Strouhal model Eq. (27) (solid line), and to the complete model obtained by combining Eqs. (8) and (12) with $h/a = 2$ (dashed line).

5. Conclusion

Two different asymptotic absorption regimes for perforates were analyzed as a function of the Strouhal number. In both low and high Strouhal limits, it has been shown that the optimal bias flow velocity yielding maximum absorption is solely fixed by the plate porosity. Analytical expressions were determined in these regimes for the optimal bias flow velocity, which does not depend on frequency. It was then demonstrated that it is possible to adjust the back cavity depth independently of the bias flow velocity to cancel the reflection coefficient. The high Strouhal regime is characterized by a Helmholtz resonance at the design point. A perforated plate operating in this regime is capable of damping a particular frequency, and features a very short resonant back cavity. However, the absorption bandwidth around the peak absorption frequency is narrow, and its width decreases as the Strouhal number increases. In applications where a large frequency bandwidth is required, it can be interesting to work in the low Strouhal regime. This regime features a wider absorption bandwidth, making it an attractive choice for the design of robust dampers. However, in this case, the cavity operates as a quarter-wave resonator, and thus has a larger size compared to the high Strouhal optimal regime.

The present analysis included as well effects of the perforated plate thickness, but it is worth recalling that the results found are limited to perforated plates of small porosity submitted to small acoustic disturbances. Non-linear effects associated to high sound levels may alter the perforated plate response [20]. Interactions between neighboring holes may also reduce the damping performance when the plate porosity is too high [15,16]. Predictions in the two asymptotic regimes identified in this study were compared to experimental data available in the literature and showed good agreement, validating the analysis. Results presented here may be use to ease the design of robust dampers.

Acknowledgements

This work is supported by the Direction générale de l'armement (DGA) in the form of a PhD fellowship for Alessandro Scarpato.

References

[1] I.J. Hughes, A.P. Dowling, The absorption of sound by perforated linings, Journal of Fluid Mechanics 218 (1990) 299–335.
[2] N. Tran, S. Ducruix, T. Schuller, Damping combustion instabilities with perforates at the premixer inlet of a swirled burner, Proceedings of the Combustion Institute 32 (2009) 2917–2924.
[3] D. Lörstad, J. Pettersson, A. Lindholm, Emission reduction and cooling improvements due to the introduction of passive acoustic damping in an existing SGT-800 combustor, in: Proceedings of ASME Turbo Expo 2009, GT2009-59313.
[4] G.A. Richards, D.L. Straub, E.H. Robey, Passive control of combustion dynamics in stationary gas turbines, Journal of Propulsion and Power 19 (2003) 795–810.
[5] U. Ingard, H. Ising, Acoustic nonlinearity of an orifice, Journal of the Acoustical Society of America 41 (1967) 1582–1583.
[6] A. Cummings, W. Eversman, High amplitude acoustic transmission through duct terminations: Theory, Journal of Sound and Vibration 91 (1983) 503–518.
[7] A. Cummings, Transient and multiple frequency sound transmission through perforated plates at high amplitude, Journal of the Acoustical Society of America 79 (1986) 942–951.
[8] A. Cummings, Acoustic nonlinearities and power losses at orifices, AIAA Journal 22 (1984) 786–792.
[9] T.H. Melling, The acoustic impedance of perforates at medium and high sound pressure levels, Journal of Sound and Vibration 29 (1973) 1–65.
[10] M.S. Howe, On the theory of unsteady high Reynolds number flow through a circular aperture, Proceedings of the Royal Society 366 (1979) 205–223.
[11] I.D.J. Dupère, A.P. Dowling, The absorption of sound near abrupt axisymmetric area expansions, Journal of Sound and Vibration 239 (2001) 709–730.
[12] X. Jing, X. Sun, Effect of plate thickness on impedance of perforated plates with bias flow, AIAA Journal 38 (2000) 1573–1578.

[13] K.S. Peat, R. Sugimoto, J.L. Horner, The effects of thickness on the impedance of a rectangular aperture in the presence of a grazing flow, Journal of Sound and Vibration 292 (2006) 610–625.
[14] S.M. Grace, K.P. Horan, M.S. Howe, The influence of shape on the Rayleigh conductivity of a wall aperture in the presence of grazing flow, Journal of Fluids and Structures 12 (1998) 335–351.
[15] S.-H. Lee, J.-G. Ih, K.S. Peat, A model of acoustic impedance of perforated plates with bias flow considering the interaction effect, Journal of Sound and Vibration 303 (2007) 741–752.
[16] R. Tayong, T. Dupont, P. Leclaire, Experimental investigation of holes interaction effect on the sound absorption coefficient of micro-perforated panels under high and medium sound levels, Applied Acoustics 72 (2011) 777–784.
[17] J. Dassé, S. Mendez, F. Nicoud, Large-eddy simulation of the acoustic response of a perforated plate, in: 14th AIAA/CEAS Aeroacoustics Conference, AIAA Paper 2008-3007.
[18] M.S. Howe, Acoustics of Fluid–Structure Interactions, Cambridge University Press, Cambridge, 1998.
[19] V. Bellucci, P. Flohr, C. Paschereit, Numerical and experimental study of acoustic damping generated by perforated screens, AIAA Journal 42 (2004) 1543–1549.
[20] A. Scarpato, S. Ducruix, T. Schuller, A LES based sound absorption analysis of high-amplitude waves through an orifice with bias flow, in: Proceedings of ASME Turbo Expo 2011, GT2011-45639, 2011.
[21] J. Rupp, J. Carrotte, M. Macquisten, The use of perforated damping liners in aero gas turbine combustion systems, in: Proceedings of ASME Turbo Expo 2011, GT2011-45488.
[22] A. Scarpato, N. Tran, S. Ducruix, T. Schuller, Modeling the damping properties of perforated screens traversed by a bias flow and backed by a cavity at low Strouhal number, Journal of Sound and Vibration 331 (2012) 276–290.
[23] C.L. Morfey, Acoustic energy in non-uniform flows, Journal of Sound and Vibration 14 (1971) 159–170.
[24] D.W. Bechert, Sound absorption caused by vorticity shedding, demonstrated with a jet flow, Journal of Sound and Vibration 70 (1980) 389–405.
[25] J.W.S. Rayleigh, The Theory of Sound, MacMillan, London, 1896.
[26] A.P. Dowling, I.J. Hughes, Sound absorption by a screen with a regular array of slits, Journal of Sound and Vibration 156 (1992) 387–405.
[27] S. Barbosa, P. Scouflaire, S. Ducruix, Time resolved flowfield, flame structure and acoustic characterization of a staged multi-injection burner, Proceedings of the Combustion Institute 32 (2009) 2965–2972.
[28] F. Boudy, D. Durox, T. Schuller, S. Candel, Nonlinear mode triggering in a multiple flame combustor, Proceedings of the Combustion Institute 33 (2011) 1121–1128.